

ture averaged over the Northern Hemisphere land is 0.7 K higher for June to August 9000 years B.P. The global average increase of surface temperature is only 0.2 K because the 0.7 K increase of land surface temperature is averaged with zero change for ocean surface temperature (Table 2).

The simulated intensification of the Northern Hemisphere summer monsoon agrees with paleoclimatic evidence in Africa and the Middle East of enlarged lakes during early Holocene time (1). Hydrological and energy balance studies of enlarged paleolakes of West Africa, East Africa, and northwest India yield estimates of precipitation increases (compared to modern values) of 20 to 100 percent (12). The results of this experiment for 9000 years B.P. are in fair agreement with other results based on records of lake levels, alluvial records, pollen records of more mesic vegetation types, and ocean core records of monsoon-related upwelling (13). The model results are also of interest for studies of the cultural history of Africa and the Near East in early Holocene time (14).

The period of enlarged paleolakes is restricted to 10,000 to 5000 years B.P. (1). This interval corresponds roughly with the interval of increased solar radiation for Northern Hemisphere summer, which peaked around 10,000 to 9000 years B.P. and returned close to modern values by 5000 years B.P. (6). A previous interval of high lake levels at 30,000 to 25,000 years B.P. (1) corresponds with a solar radiation regime that is similar to the pattern for 9000 years B.P. at tropical latitudes because of the approximate 21,000-year period of the precession cycle (6).

The opposite segment of the seasonal solar radiation cycle of 9000 years B.P. (December, January, and February) also influences the simulated climate. During January 9000 years B.P. the solar radiation is 7 percent less than at present over a broad latitudinal band and, in the simulation experiment, the land cools relative to the ocean. Because of compensating effects of the seasonal radiation extremes, a full annual-cycle simulation is required in order to summarize the climate's sensitivity to orbital parameter changes (Table 2) (15). The annual and global average values for surface temperature and pressure do not change.

Evidence for important feedback relations between ocean, atmosphere, and ice sheets on the time scale of the orbital variations (10) has been ignored in this experiment, as have possible land surface or CO₂ feedbacks (16). Including these factors in models, repeating the

sensitivity experiment with different models, and conducting detailed validation studies (17) remain tasks for the future.

JOHN E. KUTZBACH

Center for Climatic Research and
Department of Meteorology, University
of Wisconsin, Madison 53706

References and Notes

1. F. A. Street and A. T. Grove, *Quat. Res. (N.Y.)* 12, 83 (1979); W. L. Prell *et al.*, *ibid.* 14, 309 (1980).
2. J. D. Hays, J. Imbrie, N. J. Shackleton, *Science* 194, 1121 (1976); J. Imbrie and J. Z. Imbrie, *ibid.* 207, 943 (1980).
3. M. J. Suarez and I. M. Held, *Nature (London)* 263, 46 (1976); *J. Geophys. Res.* 84, 4825 (1979); S. H. Schneider and S. L. Thompson, *Quat. Res. (N.Y.)* 12, 188 (1979).
4. M. Milankovitch, *K. Serb. Akad. Beogr. Spec. Publ. 132* (1941) (translated by the Israel Program for Scientific Translations, Jerusalem, 1969).
5. F. E. Zeuner, *The Pleistocene Period—Its Climate, Chronology, and Faunal Successions* (Hutchinson, London, 1959); W. L. Prell, abstract, 61st annual meeting of the American Meteorological Society, San Diego, Calif., 19 to 22 January 1981; R. A. Bryson and A. M. Swain, *Quat. Res. (N.Y.)*, in press; B. J. Mason, *Q. J. R. Meteorol. Soc.* 102, 473 (1976). The Mason article contains a report by A. Gilchrist on a climate model experiment for May and June 10,000 years B.P. where the simulated climate was warmer than present.
6. A. L. Berger, *Quat. Res. (N.Y.)* 9, 139 (1978); E. Hopkins, thesis, University of Wisconsin, Madison (1981). An algorithm developed by Hopkins was used to produce Table 1 and to calculate the solar radiation for the experiment. The solar radiation values in Table 1 are averages for the entire month and differ somewhat from mid-month values calculated by Berger. These solar radiation values were calculated for calendar dates relative to a vernal equinox that was fixed at 21 March. Because of the slight difference in eccentricity between 9000 years B.P. and the present, global average and annual average solar radiation was 0.005 percent higher then. Using the estimate that a 1 percent change of solar constant produces a 1.8 K change of temperature [R. T. Wetherald and S. Manabe, *J. Atmos. Sci.* 32, 2044 (1975)], a global average temperature increase for 9000 years B.P. (relative to the present) of about 0.01 K is expected.
7. B. L. Otto-Bliesner, thesis, University of Wisconsin, Madison (1980); G. W. Branstator, D. D. Houghton, *J. Atmos. Sci.*, in press.
8. W. L. Gates, *Science* 191, 1138 (1976); *J. Atmos. Sci.* 33, 1844 (1976); S. Manabe and D. G. Hahn, *J. Geophys. Res.* 82, 3889 (1977); J. Williams, R. Barry, W. Washington, *J. Appl. Meteorol.* 13, 305 (1974).
9. CLIMAP Project Members, *Science* 191, 1131 (1976).
10. W. F. Ruddiman and A. McIntyre, *Quat. Res. (N.Y.)* 3, 117 (1973); *Science* 212, 617 (1981). Studies of the observational record from ocean cores will be needed to test the assumption that ocean temperatures at 9000 years B.P. were near modern values.
11. R. A. Bryson, W. M. Wendland, J. D. Ives, J. T. Andrews, *Arct. Alp. Res.* 1, 1 (1969); H. H. Lamb, *Climate: Present, Past and Future*, vol. 2, *Climatic History and the Future* (Methuen, London, 1977).
12. J. E. Kutzbach, *Quat. Res. (N.Y.)* 14, 210 (1980); A. Swain, J. Kutzbach, S. Hastenrath, in preparation.
13. K. W. Butzer, G. L. Isaac, J. L. Richardson, C. Washbourn-Kamau, *Science* 175, 1069 (1972); F. A. Street, *Palaeoecol. Afr.* 11, 135 (1979); G. Wickens, *Boissiera* 24, 43 (1975); J. Maley, *Nature (London)* 269, 573 (1977); G. Singh, R. D. Joshi, A. B. Singh, *Quat. Res. (N.Y.)* 2, 496 (1972); D. A. Adamson, F. Gasse, F. A. Street, M. A. J. Williams, *Nature (London)* 287, 50 (1980); W. L. Prell, abstract, NATO Conference on "Coastal Upwelling: Its Sediment Record," Vilamoura/Algarve, Portugal, September 1981.
14. K. W. Butzer, *Environment and Archeology: An Ecological Approach to Prehistory* (Aldine-Atherton, Chicago, 1971).
15. J. E. Kutzbach and B. L. Otto-Bliesner are preparing a complete report on this sensitivity experiment for an entire seasonal cycle.
16. S. L. Thompson and S. H. Schneider, *Nature (London)* 290, 9 (1981).
17. G. M. Peterson, T. Webb III, J. E. Kutzbach, T. van der Hammen, T. A. Wijmstra, F. A. Street, *Quat. Res. (N.Y.)* 12, 47 (1979).
18. Research grants ATM79-16443 and ATM79-26039 to the University of Wisconsin, Madison, from the National Science Foundation's Climate Dynamics Program supported this work. I thank B. Otto-Bliesner for collaboration in the use of the low-resolution general circulation model, P. Guetter for performing the computations, and E. Hopkins for the algorithm used to calculate the solar radiation for 9000 years B.P. The computations were made at the National Center for Atmospheric Research (NCAR), Boulder, Colo., with a computing grant from the NCAR Computing Facility.

15 May 1981; revised 27 July 1981

Chlorine Monoxide Radical, Ozone, and Hydrogen Peroxide: Stratospheric Measurements by Microwave Limb Sounding

Abstract. Profiles of stratospheric ozone and chlorine monoxide radical (ClO) have been obtained from balloon measurements of atmospheric limb thermal emission at millimeter wavelengths. The ClO measurements, important for assessing the predicted depletion of stratospheric ozone by chlorine from industrial sources, are in close agreement with present theory. The predicted decrease of ClO at sunset was measured. A tentative value for the stratospheric abundance of hydrogen peroxide was also determined.

As part of NASA's Upper Atmosphere Research Program, we have developed a balloon-borne microwave limb sounder (BMLS) to perform measurements of the earth's stratosphere. The BMLS is tuned to simultaneously measure thermal emission in three spectral bands near 205 GHz (wavelength, 1.5 mm), where rotational lines of ClO, O₃, and H₂O₂ occur. This choice for initial tuning was based on the need for more

measurements of ClO to help understand the catalytic depletion of stratospheric O₃ by chlorine from industrial sources (1). The nearby H₂O₂ band was included because stratospheric H₂O₂, for which no measurements have yet been reported, may be important in O₃ - HO_x chemistry. Our first flight with the BMLS was from the National Scientific Balloon Facility in Palestine, Texas (32°N, 96°W), on 20 February 1981. This

report describes results from that flight.

The BMLS makes measurements looking through the limb of the earth's atmosphere from above. It is a follow on to an aircraft instrument that was used to obtain an upper limit for stratospheric ClO (2) and to measure H₂O in the stratosphere and mesosphere (3) and in the Orion Nebula (4). From a balloon, the stratospheric ClO signal is approximately five times larger than from aircraft and approximately 30 times larger than from the ground. The observation geometry also provides better vertical resolution than obtained in ground and aircraft measurements because a narrow field of view can be scanned through the atmospheric limb. Additional information on the vertical distribution of species is obtained independently from the shape of the pressure-broadened line, as is done for aircraft and ground-based measurements.

Three filter banks perform spectral analysis of the signal. Each covers about 300 MHz and contains 9 filters with 32-

MHz resolution, 13 with 8-MHz resolution, and 13 with 2-MHz resolution. No spectral scanning is required. The center frequencies of the three banks are set at 204.352, 204.574, and 206.132 GHz, the respective laboratory-measured frequencies of ClO, H₂O₂, and O₃ lines (5). Within each bank the set of filters with a given resolution is centered on the line; adjacent filters have responses that overlap, approximately, at their half-power points. This filter arrangement provides a spectral zoom effect, which gives better resolution near line center. The filter outputs are detected, digitized, and telemetered to ground for processing.

The 205-GHz heterodyne radiometer has a second-harmonic Schottky diode mixer (6) and a 104-GHz klystron local oscillator phase-locked to a crystal reference. The first heterodyne down-conversion is to 4-GHz intermediate frequency for the ClO and H₂O₂ bands and to a 2-GHz intermediate frequency for the O₃ band.

The antenna system is an offset Casse-

grain system with a main reflector 50 cm in diameter. The input optics to the mixer select a highly tapered spatial mode, which gives good antenna beam efficiency. The measured beam width (full angular width between half-power points) is 0.3°, the highest sidelobe is at -26 dB, and the antenna beam efficiency (fraction of isotropic signal received within 2.5 times the half-power beam width) is 0.99. The antenna beam width corresponds to a vertical range of less than 3 km at the tangent point of all our stratospheric observation paths. A flat mirror in front of the main reflector scans the antenna beam through the atmospheric limb for profile measurements. This mirror is programmably stepped through a subset of 64 discrete positions during measurements. A 10-cm mirror near the antenna system focus chops the input to the radiometer at 4 Hz between the limb radiation received by the antenna and a 50° elevation sky reference. The switching mirror can also chop the radiometer input between a blackbody target and sky reference for in-flight calibration. The absolute calibration accuracy is 5 percent or better.

The instrument performed perfectly during the 10-hour flight. Useful data were obtained between 12:30 p.m., when the balloon reached float altitude of ~39 km, and 6:30 p.m., when the balloon had descended to ~37 km. During the entire flight the balloon remained within 200 km of its launch point. Pointing in the vertical plane was checked by a ten-position scan through the tropopause that measured the increase in H₂O emission there. The pointing determined in this way agreed within 0.1° of the absolute pointing to which the BMLS had been aligned. The uncertainty is due to uncertainties in the upper tropospheric water vapor distribution measured by nearby radiosondes; it introduces a vertical uncertainty < 1 km in the stratospheric layers to which the instrument points for profile measurements.

Radiometric calibrations were performed approximately every 1/2 hour during the flight. Overall gain changed by less than 1 percent between calibrations and by less than 4 percent throughout the flight. While the balloon was above 37 km six scans through the limb, each requiring approximately 1/2 hour, were performed. During the other 3 hours the scan mirror was commanded to hold the field of view at -3.3° elevation for a more accurate ClO measurement around 30 km.

Figure 1 shows the O₃ and ClO emission lines measured at three elevation angles. A small slope of 0.3 K over 300

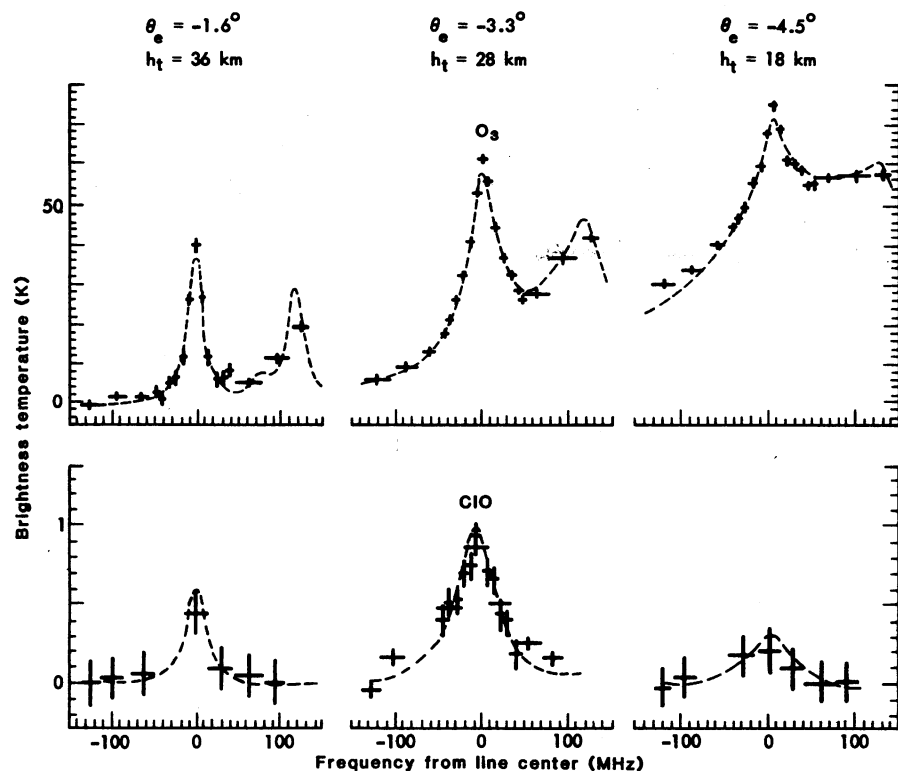


Fig. 1. The O₃ and ClO emission lines measured at three elevation angles θ_e . The tangent height h_t of the observation path is also given. The vertical scale is the brightness (equivalent blackbody) temperature of the received power. Measurements are indicated by crosses, whose vertical extent is twice the standard deviation of the measurement noise and whose horizontal extent is the spectral resolution. Dashed curves are emission lines calculated for the retrieved profiles shown in Fig. 2a. The discrepancy between measurement and calculation at O₃ line center exists because we did not attempt to determine O₃ values above 39 km but used a standard profile there. The O₃ line centered in the band is the 24_{5,19} → 25_{4,22} GHz transition at 206.132 GHz. The O₃ line near the right edge of the band is the 9_{3,7} → 10_{2,8} transition at 210.803 GHz, which occurs in the image sideband. The small bump between these two lines in the calculated O₃ spectrum for $\theta_e = -1.6^\circ$ is the 2_{2,0} → 3_{1,3} transition at 210.762 GHz. The ClO line is the 11/2 → 9/2 transition at 204.352 GHz. The measured instrument sideband responses (< -20 dB for the ClO band and -3 dB for the O₃ band) were included in the calculations.

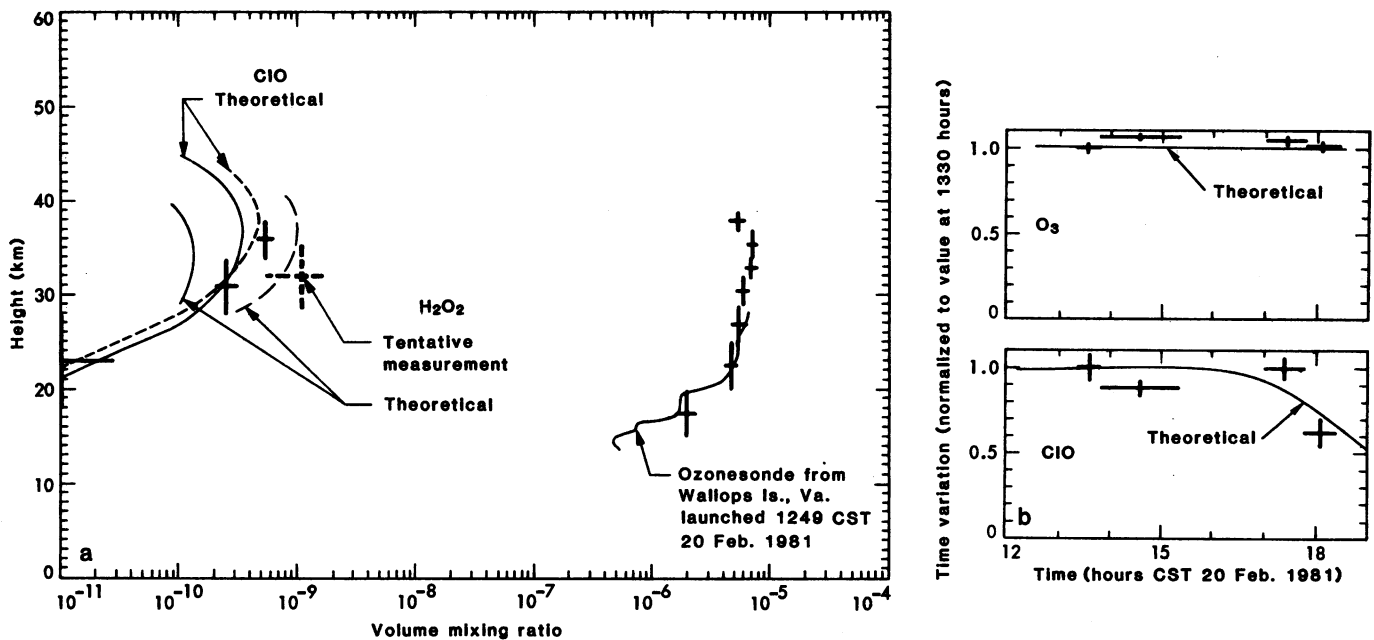


Fig. 2. (a) Profiles of ClO and O₃ and tentative value for H₂O₂ obtained from the BMLS measurements between 1300 and 1600 central standard time (CST) on 20 February 1981 (+), and recent theoretical ClO and H₂O₂ profiles from the steady-state calculations of Crutzen (12) (dashed lines) and from the time-dependent calculations of Chang (11) (solid lines) for 1400 hours at equinox. The BMLS ClO value at 18 to 28 km is an upper limit. Also shown are measurements from an ozonesonde launched from Wallops Island, Virginia (38°N, 76°W), at the same time as the BMLS flight. (b) Time variation of O₃ and ClO. The crosses give the area under the measured emission lines at - 3.3° elevation normalized to the value at 1330 hours. This quantity is proportional to the number of molecules between ~ 27 and 35 km (sunset at these altitudes occurred at ~ 1830 hours). The theoretical curves give the predicted variation in the number of molecules between 27 and 35 km from the time-dependent calculations of Chang (11), who used the rates recommended in (15).

MHz has been removed from the ClO data; otherwise the values shown were obtained directly from the instrument. The line at 204.352 GHz is assigned to ClO because it occurs at exactly the frequency of the 11/2 → 9/2 ³⁵ClO transition. We investigated the possibility that other atmospheric spectral lines occur at this frequency. The only possibility we found was that an O₃ line with rotational quantum number greater than 40 might occur at the ClO frequency. However, the 204.352-GHz line cannot be due to O₃ since its measured angular and time variation is inconsistent with the O₃ profile and variation simultaneously measured with the 206.132-GHz O₃ line. We thus conclude that the 204.352-GHz line is from ClO.

Our measurements also show a spectral feature at the correct frequency for the H₂O₂ line to which the BMLS was tuned. The integrated strength of this line, from recent spectroscopic data (7), corresponds to an H₂O₂ abundance of 1.1 ± 0.5 parts per billion by volume in a layer between ~ 27 and ~ 35 km. However, as we have not yet demonstrated that the BMLS H₂O₂ band is free of spurious responses and the signal-to-noise ratio is only about 2 standard deviations, we report the H₂O₂ measurement as tentative at this time.

Figure 1 also shows the calculated O₃ and ClO spectral lines for the profiles

retrieved from the BMLS data. The radiative transfer calculations for these signals were performed as described previously (2) and the model of atmospheric temperature and pressure at 30°N in January (8) was used. Measurements made on the day of the flight by radiosondes from six stations within range of the BMLS field of view showed that the stratospheric temperature profile differed from this model by less than 4 K. Such a small difference has negligible effect on our calculations and retrievals. Hyperfine components of the ClO line were included in the calculations, and the N₂-broadened ClO line width parameter recently measured in our laboratory was used (9). The N₂-broadened O₃ line width parameter recently measured at the Laboratoire de Spectroscopie Hertzienne of the Université de Lille (10) was used with a $T^{-0.7}$ temperature dependence. Line strengths used in the calculations are documented in (5). We consider these line strengths accurate to 1 percent.

The profiles of ClO and O₃ and the tentative value for H₂O₂ retrieved from the BMLS measurements are shown in Fig. 2a. These were obtained by first calculating the partial derivatives of the BMLS observables with respect to the profile points. The partial derivatives were then used to determine the profile values that give the best least-squares fit

to BMLS measurements. This procedure uses the information on vertical distribution contained in both the limb scan and the spectral line shape. The vertical extent of the profile points was chosen to be somewhat larger than the instrumental resolution in order to reduce noise. Figure 2b shows the measured time variation in the O₃ and ClO signals. Small corrections for changes in balloon altitude during the measurements have been included.

Our measured ClO profile agrees closely with recent theoretical predictions by Chang (11) and Crutzen (12) shown in Fig. 2a. These calculations incorporate the recently measured (13) rate for the reaction of OH with HNO₃, which leads to a steeper ClO gradient in the lower stratosphere than was previously predicted. The measured time variation supports predictions of a decrease in lower stratospheric ClO through sunset due to formation of ClONO₂ at night. Our tentative H₂O₂ value is closer to the calculations of Crutzen, who used a higher rate for the formation of H₂O₂ by recombination of HO₂ (14), than to the calculations of Chang, who used the rates recommended by NASA in January 1981 (15). Our measured O₃ profile agrees well with the profile measured at the same time by an ozonesonde at approximately the same latitude but 1500 km away.

The CIO values obtained here are consistent with the upper limit and tentative detection of our earlier summer aircraft measurements (2), the recent winter ground-based microwave measurement (16), and the mean of winter in situ resonance fluorescence measurements (17). Our winter balloon measurement and earlier summer aircraft measurements indicate less CIO above ~ 30 km than was measured by laser heterodyne radiometry (18) in autumn and, occasionally, by resonance fluorescence in summer (17). Simultaneous measurements with our instrument and others should show whether these differences are due to natural variability or to measurement technique.

Note added in proof: A second flight of the BMLS from the National Scientific Balloon Facility was performed on 11 and 12 May 1981, and useful CIO and O₃ measurements were obtained between approximately midnight and noon. Initial analyses show that (i) before sunrise the CIO averaged over the altitude region ~ 27 to 33 km is at least ten times below its midday value, and (ii) after sunrise the CIO at ~ 27 to 33 km increased, reaching a value by 11 a.m. (local time) which agreed with that measured on the first BMLS flight within 20 percent. These initial results from the second flight further support theoretical predictions that CIONO₂ is formed from CIO in the stratosphere at night. The tentative H₂O₂ feature is still under investigation.

J. W. WATERS
J. C. HARDY
R. F. JARNOT
H. M. PICKETT

Earth and Space Sciences Division
and Observational Systems Division,
Jet Propulsion Laboratory,
California Institute of Technology,
Pasadena 91109

References and Notes

1. M. J. Molina and F. S. Rowland, *Nature (London)* **249**, 810 (1974); R. S. Stolarski and R. J. Cicerone, *Can. J. Chem.* **52**, 1610 (1974); J. A. Logan, M. J. Prather, S. C. Wofsy, M. B. McElroy, *Philos. Trans. R. Soc. London Ser. A* **290**, 187 (1978); P. J. Crutzen, I. S. A. Isaksen, J. R. McAfee, *J. Geophys. Res.* **83**, 345 (1978); *NASA Ref. Publ.* 1049 (1979); Y. L. Yung, J. P. Pinto, R. T. Watson, S. P. Sander, *J. Atmos. Sci.* **37**, 339 (1980).
2. J. W. Waters, J. J. Gustincic, R. K. Kakar, H. K. Roscoe, P. N. Swanson, T. G. Phillips, T. deGraauw, A. R. Kerr, R. J. Mattauca, *J. Geophys. Res.* **84**, 7034 (1979).
3. J. W. Waters, J. J. Gustincic, P. N. Swanson, A. R. Kerr, in *Atmospheric Water Vapor* (Academic Press, New York, 1980), p. 229.
4. J. W. Waters, J. J. Gustincic, R. K. Kakar, T. B. H. Kuiper, H. K. Roscoe, P. N. Swanson, E. N. Rodriguez Kuiper, A. R. Kerr, P. Thaddeus, *Astrophys. J.* **235**, 57 (1980).
5. R. L. Poynter and H. M. Pickett, *Submillimeter, Millimeter, and Microwave Spectral Line Catalogue* (Publ. 80-23, Jet Propulsion Laboratory, Pasadena, Calif., 1981).

6. P. Zimmermann and R. J. Mattauca, paper presented at the Institute of Electrical and Electronics Engineers—Microwave Theory and Techniques Symposium, Orlando, Fla., December 1979.
7. P. Helminger, W. C. Bowman, F. C. DeLucia, *J. Mol. Spectrosc.* **85**, 120 (1981); E. A. Cohen and H. M. Pickett, *ibid.* **87**, 582 (1981).
8. *U.S. Standard Atmosphere Supplements, 1966* (Government Printing Office, Washington, D.C., 1966), pp. 102–105.
9. H. M. Pickett, D. E. Brinza, E. A. Cohen, *J. Geophys. Res.* **86**, 7279 (1981).
10. N. Monnanteuil, private communication.
11. J. Chang, private communication.
12. P. Crutzen, private communication.
13. P. H. Wine, A. R. Ravishankara, N. M. Kreutter, R. C. Shah, J. M. Nicovich, R. L. Thompson, *J. Geophys. Res.* **86**, 1105 (1981).
14. The rate used by Crutzen for recombination of HO₂ to form H₂O₂ is the same as that measured for the reaction of HO₂ with CIO by R. M. Stimpfle, R. A. Perry, and C. J. Howard [*J. Chem. Phys.* **71**, 5183 (1979)].
15. NASA Panel for Data Evaluation, *Chemical Kinetic and Photochemical Data for Use in Stratospheric Modeling, Evaluation Number 4* (Publ. 81-3, Jet Propulsion Laboratory, Pasadena, Calif., January 1981).
16. A. Parrish, R. L. de Zafra, P. M. Solomon, J. W. Barrett, E. R. Carlson, *Science* **211**, 1158 (1981).
17. J. G. Anderson, J. J. Margitan, D. H. Stedman, *ibid.* **198**, 501 (1977); J. G. Anderson, H. J. Grassl, R. E. Shetter, J. J. Margitan, *J. Geophys. Res.* **85**, 2869 (1980).
18. R. T. Menzies, *Geophys. Res. Lett.* **6**, 151 (1979); R. T. Menzies, C. W. Rutledge, R. A. Zanteson, D. L. Spears, *Appl. Opt.* **20**, 536 (1981).
19. We thank R. K. Kakar for initially suggesting that we attempt CIO measurements with microwaves and for initial spectroscopic calculations; F. S. Soltis, S. C. Bednarzyk, J. J. Gustincic, and P. Zimmermann for major contributions to the instrument development; many JPL personnel for additional support in developing the instrument; L. W. Lyon and R. E. Cofield for programming assistance; T. G. Phillips for loan of the klystron used on the flight; C. W. Balance for providing ozonesonde data; R. J. Mattauca for mixer diode development; the members of the National Scientific Balloon Facility who assisted in the preparation of our instrument for launch and performed the launch, telemetry, and recovery operations; J. Chang, P. Crutzen, and N. Monnanteuil for providing their unpublished results; and M. Allen, J. Chang, P. Crutzen, R. T. Watson, S. C. Wofsy, and Y. L. Yung for helpful discussions. During 2 years of this work, R.F.J. held a National Research Council resident research associateship at JPL. The research described here was carried out under contract with the National Aeronautics and Space Administration.

26 May 1981; revised 3 August 1981

Dated Rock Engravings from Wonderwerk Cave, South Africa

Abstract. Radiocarbon dates associated with engraved stones from sealed archaeological deposits at Wonderwerk Cave in the northern Cape Province indicate that rock engraving in South Africa is at least 10,000 years old.

Prehistoric rock art in South Africa is found in the form of both paintings and engravings. Rock paintings are generally found on cave and shelter walls in the coastal regions and in mountain ranges along the Great Escarpment and occasionally also as "art mobilier," such as painted stones, found in archeological deposits in southern Namibia and the

southern Cape Province. Rock paintings are infrequently found in the semiarid interior plateau regions, on cave and shelter walls in the relatively rare mountainous areas such as the Kuruman Hills. Engravings on exposed rocks scattered in the veld and on glacial pavements are clearly the most prevalent form of rock art in the interior plateau regions (1).

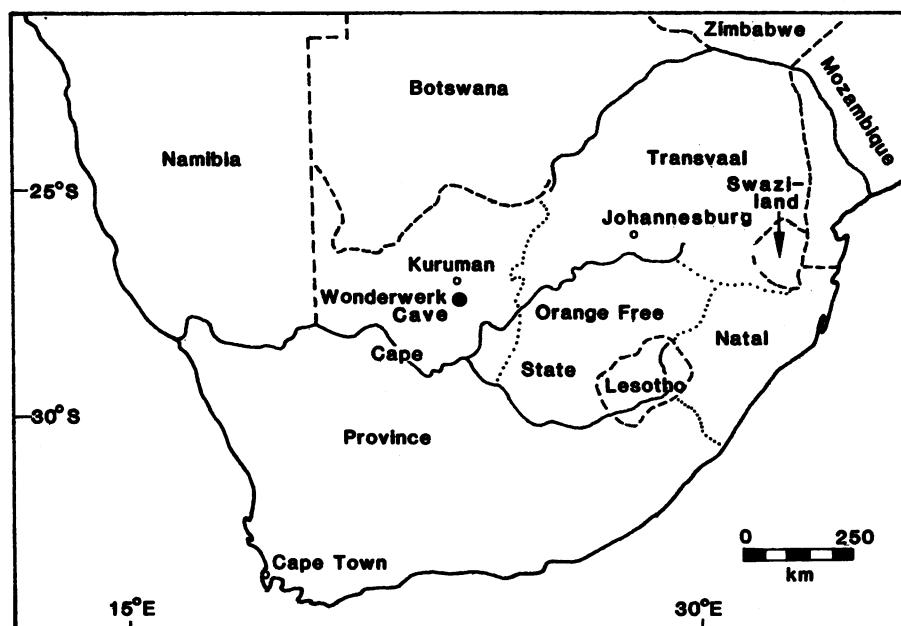


Fig. 1. Map showing the location of Wonderwerk Cave in the northern Cape Province, South Africa.